

The nlogistic-sigmoid function

Oluwasegun A. Somefun^{*1} Kayode Akingbade² and Folasade Dahunsi¹

Abstract—The variants of the logistic-sigmoid functions used in artificial neural networks are inherently, by definition, limited by vanishing gradients. Defining the logistic-sigmoid function to become n -times repeated over a finite input-output mapping can significantly reduce the presence of this limitation. Here we propose the nlogistic-sigmoid function as a generalization for the definition of logistic-sigmoid functions. Our results demonstrate that by its definition, the nlogistic-sigmoid function can reduce this vanishing of gradients, as it outperforms both the classic logistic-sigmoid function and the rectified linear-unit function in terms of learning and generalization on two representative case studies. We anticipate that this function will be the choice sigmoid activation function for deep learning.

Index Terms—Activation Functions; Vanishing Gradients; Nonlinear Functions; Neural Networks.

I. INTRODUCTION

ACTIVATION functions (AFs) follow the basis that neurons in the brain are input-output dynamic systems [1]. The choice of such computational transfer-function mappings is of critical importance in the design of any artificial neural-network (ANN) architecture, with significant control over the network's deep pattern learning ability or performance [2]–[4]. Logistic-sigmoid functions such as the standard logistic-sigmoid function (1) and the hyperbolic-tangent function (2) are common sigmoid-variant activation functions used in ANNs [3]. It can be argued that sigmoid functions are popular, partly due to the fact that their derivatives make them compatible with gradient-descent algorithms [5], [6]. In addition, they are known to possess inherent output boundedness, continuously-differentiable $C^\infty(\mathbb{R})$, smooth, monotonic and nonlinear properties [4], [7], [8] which fulfils some necessary Lyapunov stability conditions [9].

$$y = \mathbf{f}(x) = 1/(1 + e^{-x}) \quad (1)$$

$$y = \mathbf{f}(x) = \tanh(x) = (2/(1 + e^{2x})) - 1 \quad (2)$$

Therefore, logistic-sigmoid functions have found application in diverse areas, such as in physics, statistics, neuroscience, computer graphics, signal processing, feedback control and robotics. For example, the logistic-sigmoid function is the most common describing nonlinear regression function [10] for the biological baroreflex feedback regulation system in humans and animals [11]. It is also a recurring shape in nature,

^{*}This work was not supported by any organization

¹Oluwasegun Somefun osomefun@futa.edu.ng, and Folasade Dahunsi fmdahunsi@futa.edu.ng are with the Department of Computer Engineering, Federal University of Technology Akure, PMB 704 Ondo, Nigeria.

²Kayode Akingbade kfakingbade@futa.edu.ng is with the Department of Electrical and Electronics Engineering, Federal University of Technology Akure, PMB 704 Ondo, Nigeria.

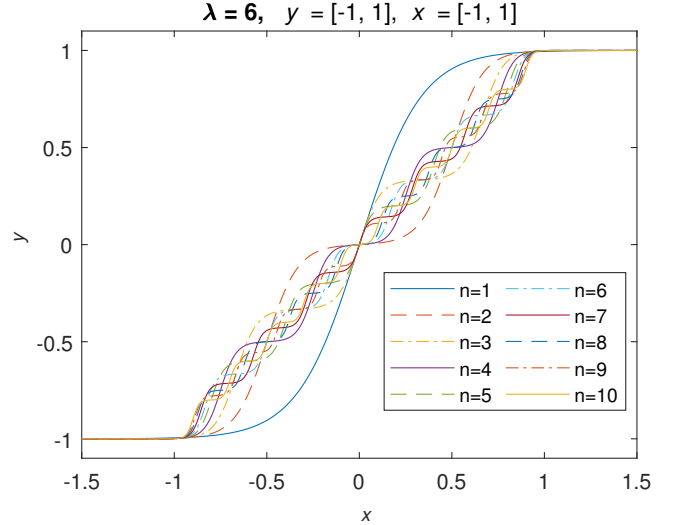


Fig. 1. The nlogistic-sigmoid, where $n = 1$ to 10, as an actuating function.

commonly observed in the motion-profile of ant swarms [12]. Further, sigmoid functions have been used to model actuating behaviours of high gain nonlinear operational amplifiers (amplifiers with saturation) [13], [14], which function as signal limiting or relay (switching) functions. It has been used to achieve smooth path-planning for mobile robots [15], and also to develop tracking-differentiators with strong nonlinear filtering properties [16].

Likewise, considerable research in the literature have been dedicated to AFs. For the application of logistic-sigmoid activation functions, see [17]–[23]. Notably, for best function approximation and faster convergence, it has been suggested that sigmoid functions should be symmetric about the origin of the function's input-output map [3]. The function approximation capability of sigmoids have also been investigated in relatively recent works. For instance, [24] using a broad class of common AFs, explored the smooth function approximation ability of deep neural networks and classified AFs into two groups: piecewise linear (rectified linear-unit (ReLU) variants) and locally quadratic (sigmoid variants). Further, for vector equalization based on recurrent neural networks (RNNs), in application to multi-path signal propagation, [9] showed that the approximate optimum AF could be realised as a sum of shifted hyperbolic tangent functions.

Nevertheless, two notable inherent drawbacks affect sigmoid functions. As the first short-coming: formulations of sigmoid functions possess a fundamental learning or optimization disadvantage in which their derivatives exponentially approach zero, especially as the network becomes deeper.

This famous problem defined as the vanishing (exponentially decreasing) gradient problem was first formally treated in [25], leading to the gradient-based Long Short-Term Memory (LSTM) recurrent neural network (RNN). More recently, this problem was also considered in [26]. Several proposals to partially overcome this issue have been explored in the literature. Reviewed in [27], some work-around solutions, apart from LSTM networks are: deep-belief networks, hessian-free optimisation, random-weight guessing and leverage of GPU-based computational power. Consequently, more research led to the proposals of different alternative activation functions such as in [26], [28]–[32]. A concise survey of these proposed AFs can be found in [33]. On the contrary, none of these AFs treat the root cause of the logistic-sigmoid’s vanishing gradient problem. Also, most of these alternative AFs are either sensitive to random weight initializations or cause more noisy outputs [26].

The second short-coming lies in the computational expensive natural exponential term e^u [2], [3], [34]. This is why, among AFs, the attractive property of low computational complexity and fast computational speed makes ReLU function variants popular as default choices in many deep neural-network architectures. Notwithstanding, sigmoid variants still stand out as the choice in architectures such as RNNs [35], [36]. Fortunately, through parallel computing techniques (such as GPU power), these computations can be made faster. Also, through the computing techniques of function approximation, reduced computational complexity can be realized in software within acceptable levels of accuracy [35], [37].

In this paper, contrasted with the above discussed approaches in the literature, we treat the first shortcoming: the vanishing gradient problem as a flaw in the logistic-sigmoid function definition. Specifically, over a finite input-output space, we introduce the **n**logistic-sigmoid function as a more general and formal definition for such logistic-sigmoids. As illustrated by the input-output mapping in Figure 1, this can be made suitable for use both as an activation and actuating function. To the best of our knowledge, this function definition has not been reported in the literature before.

In section II, we start with a preliminary discussion on the classic sigmoid function. The proposed function is then defined formally in section III. It will be shown that by its definition, the proposed function has over its input-output map, a n -times repeating gradient surface, whose maximum value is controlled by its tunable finite input-output limits and logistic growth-rate constant λ . The implication of this is that, to a large extent, the **n**logistic-sigmoid function can reduce the vanishing occurrence of its gradients. We validate this hypothesis in section IV where a neural-network model (shallow and deep) is trained to approximate the exclusive OR function and also to identify black and white digits 1 to 5. The obtained results show that the proposed function learns faster and generalises better than both the classic sigmoid function and ReLU function. Finally, in section V, this paper is concluded. Useful for library developers, an implementation of this function in MATLAB and C/C++ is provided in [38].

II. CLASSIC LOGISTIC-SIGMOID

The classic logistic-sigmoid function given by (3) involves mapping a bounded output co-domain $y \in \mathbb{R}$ in the range $[y_{\min}, y_{\max}]$, where y_{\min}, y_{\max} are the minimum and maximum bounds or asymptotes of y respectively, to an unspecified or unbounded input domain $x \in \mathbb{R}$ in the range $(-\infty, \infty)$, centered by an offset parameter $\delta \in \mathbb{R}$, and scaled by a logistic growth-rate parameter $\alpha \in \mathbb{R}$.

$$y = \mathbf{f}(x) = y_{\min} + \frac{y_{\max} - y_{\min}}{1 + e^{\pm\alpha(x-\delta)}} \quad (3)$$

The derivative g with respect to the input is also given by (4). The maximum value of the derivative \bar{g} occurs at the inflection point (mid-point), where $x = \delta$. It can be easily shown that $\bar{g} \equiv 0.25\alpha(y_{\max} - y_{\min})$. At this point the corresponding value of y is $(y_{\max} + y_{\min})/2$.

$$g = \frac{dy}{dx} = \frac{\alpha}{y_{\max} - y_{\min}} (y - y_{\min})(y_{\max} - y) \quad (4)$$

For the standard logistic function (1), where $y_{\max} = 1$, $y_{\min} = 0$, $\alpha = 1$, and $\delta = 0$, we have $\bar{g} = 0.25$. On the other hand, for the hyperbolic tangent function (2), where $y_{\max} = 1$, $y_{\min} = -1$, $\alpha = 2$, and $\delta = 0$, we have $\bar{g} = 1$. These formulations are, therefore, limiting in the sense that: no matter the input, the maximum gradient is fixed; and also the gradient exponentially decreases to zero as the value of the input x deviates from the δ midpoint.

These two problems can be solved to a large degree with the use of the **n**logistic-sigmoid, which features: one, a tunable logistic growth-rate constant, and two: a n -times occurring gradient map over a tunable finite input-output space (universe), such that the maximum gradient is neither too large nor too small.

III. NLOGISTIC-SIGMOID

In contrast to the classic definition, a repeating sigmoid behaviour found in the motion-profile of ant-swarms can be emulated within a defined finite input-output universe specified by $[x_{\min}, x_{\max}]$ and $[y_{\min}, y_{\max}]$.

The specified finite input and output universe (space) is partitioned into n equal sub-spaces with n inflection points at $x = \delta_i$ leading to v_i sub-sigmoids, where $i = 1, \dots, n$. This transforms the classic logistic-sigmoid function to a sum of n shifted sigmoids each with a continuous gradient map over the surface of the input-output universe.

The interval spacing for each sub-sigmoid partition in the finite input and output universe can be defined respectively as (5) and (6).

$$\Delta_x = \frac{(x_{\max} - x_{\min})}{n} \quad (5)$$

$$\Delta_y = \frac{(y_{\max} - y_{\min})}{n} \quad (6)$$

A formal definition for the periodic odd function that results from this sum of shifted sigmoids, each partition having the same property, can then be provided.

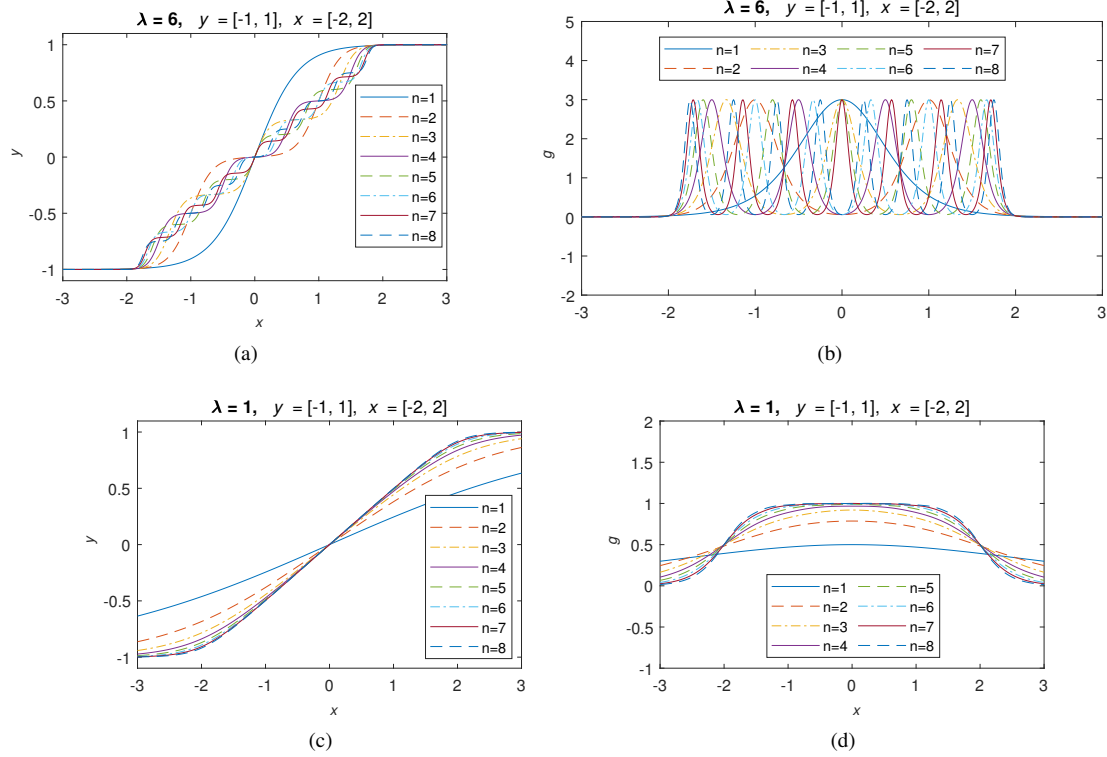


Fig. 2. output and gradient illustration of the **nlogistic-sigmoid** function as an actuating function ((a) and (b)) and as an activation function ((c) and (d)).

Definition 1. The **nlogistic-sigmoid** function, with odd output y and even output g , denoted as $\mathbf{nlsig}\pm: \mathbb{R} \rightarrow \mathbb{R}$, where $n \in \mathbb{N}^+$ and $\lim_{x \rightarrow x_{\max}} y \rightarrow y_{\max}$, $\lim_{x \rightarrow x_{\min}} y \rightarrow y_{\min}$ is:

$$\mathbf{nlsig}\pm: y = \mathbf{f}(x) = \kappa_y + \sum_{i=1}^n v_i \quad (7)$$

$$g = \tau \sum_{i=1}^n v_i (\Delta_y - v_i) \quad (8)$$

where,

$$v_i = \frac{\Delta_y}{1 + e^{\pm u}}, u = \alpha(x - \delta_i) \quad (9)$$

$$\delta_i = \kappa_x + \Delta_x \left(i - \frac{1}{2} \right) \quad (10)$$

$$\alpha = \frac{2\lambda}{\Delta_x}, \quad \tau = \frac{\alpha}{\Delta_y} \quad (11)$$

and,

$$\kappa_x = x_{\min}, \kappa_y = y_{\min}, \lambda = 6 \text{ (default)}.$$

The boundary (limit) values of the input-output universe are defined as:

$$y_{\max} = (1 - \xi) y_{\max}, \quad y_{\min} = (1 - \xi) y_{\min} \quad (12)$$

$$x_{\max} = (1 - \xi) x_{\max}, \quad x_{\min} = (1 - \xi) x_{\min} \quad (13)$$

where

$$\xi = \xi/c, \quad -c \leq \xi \leq c \quad (14)$$

and

$$c = 100 \quad \text{and} \quad \xi = 0 \text{ (default)} \quad (15)$$

with $\xi, c \in \mathbb{N}^+$, and $x, y, g, v, \alpha, \delta, \tau \in \mathbb{R}$. This completes the definition.

The parameter n defines the number of sub-sigmoids in the function, τ is the derivative constant, v_i is partial output representing the i th sub-sigmoid, u is the natural exponential input, and ξ is the limit damper constant. As an actuating function (when the input-output limits are equal), the input-output sigmoidal approximation is best achieved when the logistic growth-rate constant $\lambda = 6$. This is illustrated for an arbitrary finite input-output universe $[-1, 1]$ in Figure 1. Also as n increases in the **nlogistic-sigmoid** function, approximately linear regions around the inflection points become more evident. This behaviour offers the advantage of better function approximation as discussed in [24].

Notably, as shown by Figure 2a and Figure 2c, the logistic input-output approximation behaviour of the **nlogistic-sigmoid** function in its finite universe is dependent on λ and its input-output limits. The midpoint of the input-output limits is (\bar{x}, \bar{y}) . From (16), we see that, to ensure the curve is symmetric at a central midpoint of $\bar{\delta} = 0$, then the minimum limit must be set as $x_{\min} = -x_{\max}$ and $y_{\min} = -y_{\max}$. Figure 2b and Figure 2d illustrate that the gradient value always diminishes to zero only at the input value that maps to the maximum and minimum limits of output interval. From (17), the central inflection point $\bar{\delta}$, when n is odd is equivalent to \bar{x} . There is no central inflection point when n is even.

$$\bar{x} = \frac{x_{\max} + x_{\min}}{2}, \quad \bar{y} = \frac{y_{\max} + y_{\min}}{2} \quad (16)$$

$$\bar{\delta} = \frac{1}{n} \sum_{i=1}^n \delta_i = \bar{x} \quad (17)$$

The λ value controls the curvature of the output y and also how the gradient g and its maximum repeats itself n times at every $x = \delta_i$. It can be shown that the value of the maximum gradient \bar{g} is proportional to the value of λ and its input-output limits.

Proof. To start with, we note that the sigmoid shape repeats itself n -times in the input-output universe. It follows that, if $n > 1$, then, the maximum gradient will occur at each $x = \delta_i$, which represents the centre of each sub-sigmoid. Since, this is true, then without any loss of generality, we can assume $n = 1$. The derivative becomes:

$$g = \tau v (\Delta_y - v)$$

where

$$v = y - y_{\min}, \quad \Delta_y = y_{\max} - y_{\min}$$

At the output interval boundaries or limits, when $y = y_{\max}$ or $y = y_{\min}$, then $g = 0$.

Also, at the inflection-point (mid-point), when $x = \bar{\delta}$, the output value is $y = (y_{\max} + y_{\min})/2$, therefore,

$$g = \bar{g} = 0.5 \lambda \Delta_y / \Delta_x \quad (18)$$

When used as an actuating function, the function mapping is symmetrically centered at zero, with $x_{\max} \equiv y_{\max}$ and $x_{\min} \equiv y_{\min}$, so we have $\Delta_x = \Delta_y$, since the value of $\lambda = 6$, then the maximum gradient \bar{g} is always 3 at each midpoint $x = \delta_i$.

In contrast, for use as an activation function, the maximum gradient must be controlled by setting λ to a different value that ensures the gradient neither explodes nor vanishes. This can be achieved by normalizing λ to unity. Therefore, for use as an activation function, the default value becomes $\lambda = 1$, making the maximum gradient solely dependent on the input-output limits, as shown in (19).

$$\bar{g} = 0.5 \Delta_y / \Delta_x \quad (19)$$

This completes the proof. \square

Therefore, with the **n**logistic-sigmoid function definition, gradients do not vanish except at the input value x which maps to the maximum or minimum boundary of the output y universe. This is illustrated in Figure 2. Consequently, to a large extent, because of the way the gradient is controlled and repeated over the input-output map, the frequent occurrence of vanishing gradients in a neural network's gradient flow will be far reduced, compared to the classic sigmoid use-case.

In the next section, as proof of concept in training general multi-layer neural-network models, which are fundamental to other architectures, we empirically evaluate and compare the performance of the **n**logistic-sigmoid function to the classic logistic-sigmoid function and rectified linear-unit function.

IV. CASE STUDIES

A prevailing application of supervised machine learning using neural networks is to solve classification problems. In the literature, vanishing gradients and overfitting are chief

reasons for the poor learning performance of neural networks. This gradient is the delta of the stochastic gradient-descent (SGD) learning rule. When the gradients vanish, errors cannot be backpropagated, hence the neural network's weights cannot be trained. Vanishing gradients are often tackled by using the rectified-linear unit and advanced gradient-descent methods. In this section, we demonstrate the performance of the **n**logistic-sigmoid function in comparison with the classic sigmoid function and rectified linear-unit function as hidden activation-functions. Here, we consider two cases: a function approximation or binary classification problem and a multi-class classification problem implemented in MATLAB [2].

A shallow and deep neural-network model is constructed for both cases. For both cases, we keep the neural-network algorithms fundamental and avoid any form of "advanced" optimizations. The learning-rule by back-propagation is restricted to the vanilla first-order SGD algorithm (generalized delta rule). The learning rate for the sigmoid functions was selected to be 0.9. This was selected as 0.01 for the ReLU function in order for it to learn better. The weights ω_{ij} were randomly initialized using a zero-mean (uniform) gaussian distribution (22) at the hidden (see (20)) and output layers (see (21)), where σ is the standard deviation and η_i is the number of nodes in the adjacent i th layer [39]. For multi-output models, the vanilla log-softmax function was used as the output activation-function.

$$\sigma = \sqrt{2 / (\eta_i \cdot \eta_{i+1})} \quad (20)$$

$$\sigma = \sqrt{2 / (\eta_i + \eta_{i+1})} \quad (21)$$

$$\omega_{ij} = 2\sigma \cdot \text{rand}(\eta_i, \eta_{i+1}) - \sigma \quad (22)$$

Further, we make comments on how well the trained neural-network models: learned from the given datasets and also generalized to a test dataset for the second case-study.

A. Exclusive OR

This problem is a classical case-study for machine-learning. The objective is to learn the two binary-input "exclusive OR" logic function from a given 4×2 matrix of binary values, each with a bias of 1. This corresponds to 3 nodes at the input-layer and 1 node at the output-layer. A shallow neural-network with 4 nodes in the hidden layer was constructed. Also, a deep neural-network with 3 hidden layers and a 4–6–4 hidden node distribution was constructed. For training the neural-network, the selected number of epochs is $2^9 = 512$.

The **n**logistic-sigmoid function was configured as an hidden layer activation function using: $\lambda = 1.0$, $x_{\max} = 2.0$, $x_{\min} = -x_{\max}$, $y_{\max} = 1.0$, $y_{\min} = -y_{\max}$, and as an output layer activation function using: $\lambda = 1.0$, $x_{\max} = 2.0$, $x_{\min} = 0$, $y_{\max} = 1.0$, $y_{\min} = 0$. For both shallow and deep models $n = 1, 2, 3, 4$ was considered.

The training performance can be verified from the average training errors in Figure 3. For the shallow model, as seen in Figure 3a, the ReLU trained network settles early to a local minima, where the error was more than 10%, and similar to the classic logistic-sigmoid function trained network, it fails to converge to zero within the training time-frame. In contrast, the **n**logistic-sigmoid function trained network converges very

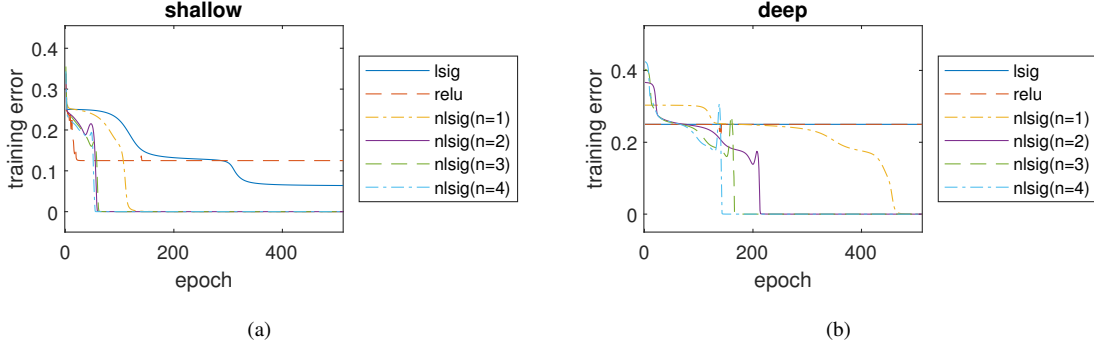


Fig. 3. exclusive OR function, average training error for the (a): shallow model, (b): deep model.

lsig		relu		lsig		relu	
0.003858	0.0002118	0.4998	0.5	0.4998	0.5	0.4998	0.5
0.9876	0.5	0.4998	0.5	0.4998	0.5	0.4998	0.5
0.9939	0.9999	0.4998	0.9999	0.4998	0.5	0.4998	0.5
0.5057	0.5	0.4998	0.5	0.4998	0.5	0.4998	0.5
nlsig (n=1)		nlsig (n=2)		nlsig (n=1)		nlsig (n=2)	
0.001693	0.0009471	0.009184	0.0006392	0.009184	0.0006392	0.009184	0.0006392
0.9985	0.999	0.9914	0.9993	0.9914	0.9993	0.9914	0.9993
0.9984	0.999	0.9898	0.9992	0.9898	0.9992	0.9898	0.9992
0.002682	0.001661	0.01166	0.0009581	0.01166	0.0009581	0.01166	0.0009581
nlsig (n=3)		nlsig (n=4)		nlsig (n=3)		nlsig (n=4)	
0.0005288	0.000341	0.0004125	0.0002944	0.0004125	0.0002944	0.0004125	0.0002944
0.9994	0.9996	0.9996	0.9997	0.9996	0.9997	0.9996	0.9997
0.9994	0.9996	0.9995	0.9996	0.9995	0.9996	0.9995	0.9996
0.0009588	0.0006573	0.0005548	0.0003674	0.0005548	0.0003674	0.0005548	0.0003674

Fig. 4. exclusive OR function, neural-network inference of the (a): shallow model, (b): deep model.

fast to zero, within the training time frame, as n is increased. Also, for the deep model, as illustrated in Figure 3a, the ReLU and classic logistic-sigmoid function trained network remained stuck in a local minima, where the error was above 20%, and failed to converge to zero within the training time-frame. In contrast, the **n**logistic-sigmoid function trained network again descended fast to zero, as n is increased, within the training time-frame. As shown in Figure 4a and in Figure 4b, only the neural-network trained with the **n**logistic-sigmoid function constantly gave accurate inference, for both the trained shallow and deep models, within the short training time-frame. The results of this case-study imply that the **n**logistic-sigmoid function can provide a faster and more accurate learning ability for trained neural-network models than both the classic-sigmoids and the ReLU function.

B. Digit Recognition

This case-study is an illustration for digit (image) recognition. As shown in Figure 5a, the training dataset is a 5×5 pixel of digits 1 to 5 with no bias. This corresponds to 25 nodes at the input-layer and 5 output-layer nodes using one-hot

encoding. The objective is to learn to recognize the first five digit characters from this minimal dataset and generalize well to a corrupted test dataset of these digits shown in Figure 5b. A shallow neural-network with 50 nodes in the hidden layer was constructed. Also a deep neural-network with 3 hidden layers and a $20 - 20 - 20$ hidden node distribution was constructed. For training the neural network, the selected number of epochs is $2^9 = 512$ for the shallow models and $2^{11} = 2048$ for the deep models.

In this case, the **n**logistic-sigmoid function was configured as an hidden layer activation function using: $\lambda = 1.0$, $x_{\max} = 4.0$, $x_{\min} = -x_{\max}$, $y_{\max} = 1.0$, $y_{\min} = -y_{\max}$. For the shallow model, $n = 1, 2, 3, 4$ were considered, while $n = 1, 2, 4, 6$ were considered for the deep model.

The training performance can be verified from the average training errors in Figure 6. For the shallow model, as seen in Figure 6a, within the training time-frame, the ReLU trained network was the slowest to converge to zero, followed by the classic logistic-sigmoid trained network, then followed by the **n**logistic-sigmoid function trained network which descended fastest to zero, as n was increased. In contrast, for the deep model, as illustrated in Figure 3a, within the training time-frame, the classic logistic-sigmoid function trained network remained stuck in a local minima, where the error was above 50%. The ReLU function trained network converged to zero faster than the **n**logistic-sigmoid function trained network when $n = 1$. As n is increased to 2 and above, the **n**logistic-sigmoid trained network, overall, converged the fastest to zero.

Using human intelligence to interpret the test data, with respect to the trained data, the following observations can be made. The first test image is more likely to be digit 1 but also has features close to digit 4. The second test image is more likely to be digit 2 but also close to digit 3. The third test image is more likely to be digit 3 but also close to digit 2. The fourth and fifth test images are clearly recognized to be digit 5, even though they differ strongly by pixels from the trained image of digit 5 with features close to digit 3.

For the shallow model, as shown in Figure 7, the classic sigmoid function trained network recognizes the first test image to be digit 1 by a probability of 18.9% or digit 4 by a probability of 54.1%, the second test image was inferred to be digit 2 by a probability of 96.5%, the third test image as digit

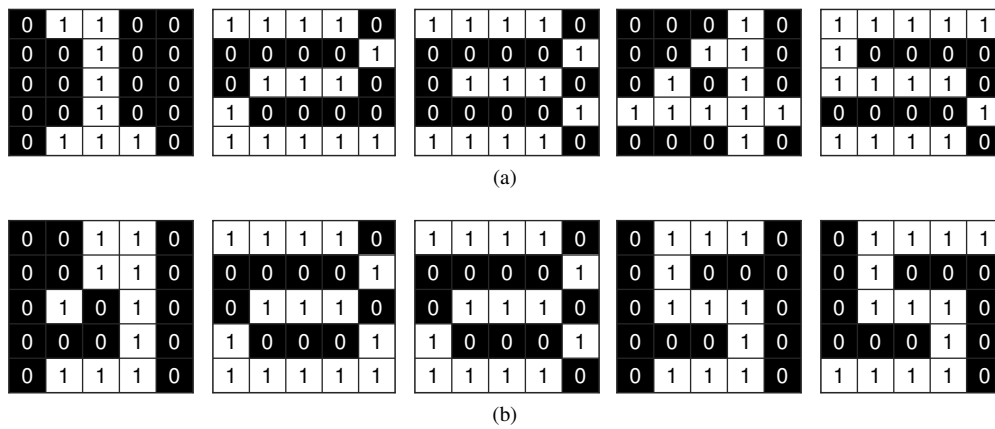


Fig. 5. 5×5 pixel (black and white) digits (a): training data, (b): test data.

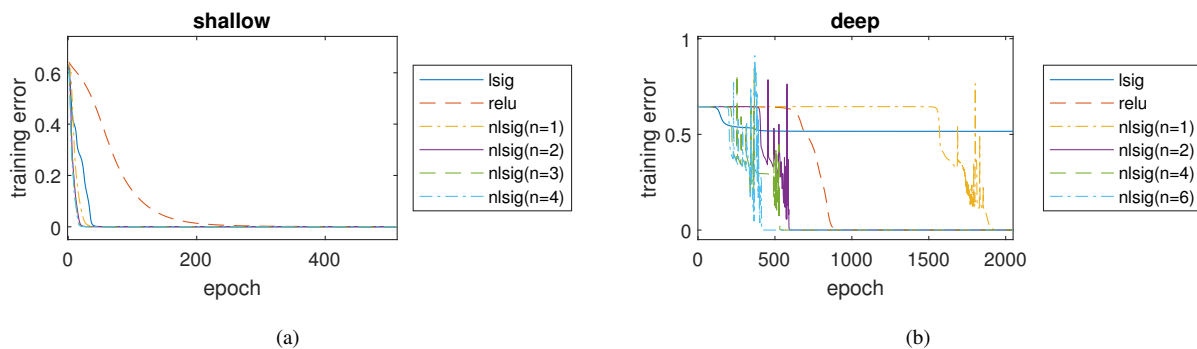


Fig. 6. 5×5 pixel digits, average training error for the (a): shallow model, (b): deep model.

3 by a probability of 95.1%, the fourth test image as digit 3 by a probability of 64.9% and the fifth test image to be digit 5 by a probability of 75.3%. The ReLU function trained network recognizes the first test image to be digit 1 by a probability of 16.5% or digit 4 by a probability of 59.2%, the second test image was inferred to be digit 2 by a probability of 78.2%, the third test image as digit 3 by a probability of 77.6%, the fourth test image as digit 1 by a probability of 25.4% or digit 3 by a probability of 38.5% and the fifth test image to be digit 5 by a probability of 55.8%. The **n**logistic-sigmoid function trained network, for all n considered, gives relatively the same inference pattern. We see that when $n = 1$, the first test image is recognized to be digit 1 by a probability of 15% or a digit 4 by a probability of 77.4%, the second test image was inferred to be digit 2 by a probability of 92.2%, the third test image as digit 3 by a probability of 90.9%, the fourth test image as digit 1 by a probability of 38.8% or digit 3 by a probability of 41.7% and the fifth test image to be digit 5 by a probability of 60.4%; then when $n = 4$, the first test image is recognized to be digit 1 by a probability of 14.5% or digit 4 by a probability of 80.5%, the second test image was inferred to be digit 2 by a probability of 94.3%, the third test image as digit 3 by a probability of 92.1%, the fourth test image as digit 1 by a probability of 44.1% or digit 3 by a probability of 39.8% and the fifth test image to be digit 5 by a probability of 57.5%.

Also, for the deep model, as illustrated in Figure 8, we observe that the classic sigmoid function trained network fails

to make any meaningful inference pattern, due to vanished gradients, except for the first test digit recognized as digit 4 by 54.5%. In contrast, for the ReLU function trained network, the first test image is recognized to be digit 4 by a probability of 60%, the second test image was inferred to be digit 2 by a probability of 97.4%, the third test image as digit 3 by a probability of 86.8%, the fourth test image as digit 5 by a probability of 89.4% and the fifth test image to be digit 5 by a probability of 92.01%. For the **n**logistic-sigmoid function trained network, we observe relatively different inference pattern as n is increased: when $n = 1$, it recognizes the first test image to be digit 1 by a probability of 56.7% or digit 4 by a probability of 43.3%, the second test image was inferred to be digit 2 by a probability of 92.2%, the third test image as digit 3 by a probability of 85.3%, the fourth test image as digit 5 by a probability of 96% and the fifth test image to be digit 5 by a probability of 81.7%; when $n = 2$, it recognizes the first test image to be digit 4 by a probability of 99.9%, the second test image was inferred to be digit 2 by a probability of 99.5%, the third test image as digit 3 by a probability of 92.1%, the fourth test image as a digit 3 by a probability of 79.3% or a digit 5 by a probability of 20.6% and the fifth test image to be a digit 3 by a probability of 62.1% or a digit 5 by a probability of 37.9%; when $n = 4$, it recognizes the first test image to be digit 1 by a probability of 99.9%, the second test image was inferred to be digit 2 by a probability of 99.8%, the third test image as digit 3 by a probability of 87.5%, the

		lsig							relu				
probability		0.1652	0.06901	0.138	0.5919	0.03602	probability		0.1885	0.0762	0.1113	0.5409	0.08307
		0.0005543	0.9645	0.03458	0.0001962	0.0001795			0.002481	0.7823	0.2051	0.00382	0.006325
		0.0004864	0.0463	0.9511	0.0003422	0.001794			0.004269	0.1988	0.7755	0.006117	0.01533
		0.147	0.1537	0.6486	0.01049	0.0402			0.2541	0.1565	0.3845	0.06681	0.1381
		0.019	0.03034	0.1933	0.004	0.7534			0.07621	0.1044	0.2298	0.03168	0.5579
		1	2	3	4	5			1	2	3	4	5
		digit							digit				
		nlsig (n=1)							nlsig (n=2)				
probability		0.1502	0.0297	0.0275	0.7741	0.01849	probability		0.1428	0.02408	0.01712	0.8018	0.01422
		0.000233	0.9221	0.07724	0.000411	1.46e-05			0.0001588	0.9375	0.06212	0.0002631	4.256e-06
		0.0006487	0.08875	0.9094	0.0009052	0.0003387			0.0004942	0.08044	0.9183	0.0006267	0.0001656
		0.3875	0.0988	0.4165	0.05593	0.04122			0.4275	0.08641	0.3993	0.05489	0.03189
		0.07778	0.01615	0.2675	0.03439	0.6042			0.08143	0.01056	0.2755	0.03922	0.5933
		1	2	3	4	5			1	2	3	4	5
		digit							digit				
		nlsig (n=3)							nlsig (n=4)				
probability		0.1423	0.02267	0.01389	0.8081	0.01304	probability		0.1451	0.02279	0.01371	0.8054	0.01296
		0.0001391	0.9421	0.05751	0.0002095	2.641e-06			0.0001276	0.9427	0.05699	0.000179	2.074e-06
		0.0004516	0.07859	0.9203	0.000517	0.0001283			0.0004257	0.0777	0.9213	0.0004571	0.000113
		0.4426	0.08276	0.3924	0.05341	0.02882			0.4406	0.08149	0.3984	0.05186	0.0277
		0.0815	0.008866	0.2831	0.0405	0.586			0.08008	0.008319	0.2964	0.03996	0.5753
		1	2	3	4	5			1	2	3	4	5
		digit							digit				

Fig. 7. test inference of the shallow neural-network model for the 5×5 pixel digits.

		lsig							relu				
probability		0.1207	0.1108	0.1075	0.5448	0.1162	probability		0.01104	8.159e-07	0.01379	0.3755	0.5996
		0.2	0.1999	0.1999	0.2002	0.1999			3.492e-18	0.9735	0.02649	9.176e-07	5.568e-08
		0.2	0.1999	0.1999	0.2002	0.1999			3.978e-14	0.1315	0.8683	7.442e-05	4.193e-05
		0.1999	0.1999	0.1999	0.2003	0.1999			0.0003999	6.911e-07	0.0915	0.01436	0.8937
		0.1999	0.1999	0.1999	0.2002	0.1999			0.0001438	1.143e-07	0.07515	0.004645	0.9201
		1	2	3	4	5			1	2	3	4	5
		digit							digit				
		nlsig (n=1)							nlsig (n=2)				
probability		0.5672	4.478e-12	4.526e-12	0.4328	6.113e-07	probability		0.0003778	1.474e-14	4.674e-12	0.999	0.0005916
		6.903e-14	0.9216	0.07836	7.034e-15	1.625e-08			9.265e-13	0.9954	0.004552	1.394e-16	2.203e-12
		2.68e-11	0.1466	0.8533	2.229e-10	7.924e-05			1.026e-10	0.07901	0.921	2.02e-11	5.308e-07
		8.873e-07	1.487e-05	0.03604	0.003705	0.9602			1.541e-07	3.673e-05	0.7934	0.0002855	0.2063
		1.482e-08	3.382e-05	0.1831	0.0001533	0.8167			1.111e-09	3.304e-07	0.621	4.926e-05	0.379
		1	2	3	4	5			1	2	3	4	5
		digit							digit				
		nlsig (n=4)							nlsig (n=6)				
probability		0.9998	1.544e-05	3.305e-09	0.0002307	2.325e-06	probability		1.4e-05	4.899e-09	0.0002092	0.9998	6.703e-06
		4.049e-06	0.9982	0.001768	2.124e-12	4.653e-08			2.863e-06	0.9411	0.05885	1.577e-05	4.886e-05
		2.392e-06	0.1246	0.8754	3.338e-10	5.237e-05			1.749e-10	4.27e-05	0.9999	2.154e-05	4.159e-05
		0.1283	5.608e-05	0.001649	0.01698	0.8531			1.124e-05	0.0002525	0.08074	1.03e-05	0.919
		3.694e-07	4.807e-10	0.0003626	8.94e-05	0.9995			3.229e-06	2.697e-05	0.0001202	2.712e-09	0.9998
		1	2	3	4	5			1	2	3	4	5
		digit							digit				

Fig. 8. test inference of the deep neural-network model for the 5×5 pixel digits.

fourth test image as a digit 5 by a probability of 85.3% and the fifth test image to be digit 5 by a probability of 99.9%; when $n = 6$, it recognizes the first test image to be digit 4 by a probability of 99.9%, the second test image was inferred to be digit 2 by a probability of 94.1%, the third test image as digit 3 by a probability of 99.9%, the fourth test image as a digit 5 by a probability of 91.9% and the fifth test image to be digit 5 by a probability of 99.9%.

From these statistics, we conclude that in descending order of performance, the $n = 4$, $n = 1$, $n = 6$ nlogistic-sigmoid function trained deep networks and the ReLU trained deep network gave the closest inferences similar to the human observation. Overall, for both the shallow and deep neural-network models, the nlogistic-sigmoid function trained networks, followed by the ReLU trained networks, resulted in faster learning, more accurate inference, and less overfitting. These results connote that the nlogistic-sigmoid function can give a more generalized pattern learning ability, or in other words, a less-overfitted neural network model than both the classic-sigmoids and the ReLU functions.

C. Remarks

The two case-studies demonstrate vividly that in contrast to the current dominant belief, the logistic-sigmoid function can indeed be used for learning in the hidden layers of deep neural-networks without the problem of the gradients vanishing or exploding. The vanishing gradient problem was essentially just a definition problem with the classic logistic-sigmoids, which is resolved as shown in this paper, by the definition of the input-output bounded nlogistic-sigmoid function.

Finally, we note that the second short-coming of the proposed function, that is, the increased arithmetic and exponential operations remain, even as the n parameter is increased. Notwithstanding this short-coming, satisfactory computational-speed and accuracy can be obtained from computing the natural exponential term by using a combination of function approximation techniques involving ones-normalization, bit-manipulation and exponentiation-by-squaring.

V. CONCLUSIONS

In this paper, the nlogistic-sigmoid function was defined and introduced for use as an actuating and activating function. It generalised the classic logistic-sigmoid function to a function of n sigmoids over a defined finite input-output map. It was shown that this function inherently overcomes to a large extent the famous vanishing-gradient problem of sigmoid functions, hence would significantly benefit deep learning. We expect that this function will also become a candidate replacement for the classic logistic-sigmoid functions in other applications (such as in reward functions or fuzzy membership functions).

AUTHOR CONTRIBUTIONS

The corresponding author is O.A. Somefun. The research in this paper was jointly supervised by K.F. Akingbade and F.M. Dahunsi.

DECLARATION OF INTERESTS

The authors declare no competing interests.

REFERENCES

- [1] Sze, V., Chen, Y., Yang, T. & Emer, J. S. Efficient Processing of Deep Neural Networks: A Tutorial and Survey. *Proceedings of the IEEE* **105**, 2295–2329 (2017).
- [2] Kim, P. *MATLAB Deep Learning: With Machine Learning, Neural Networks and Artificial Intelligence* (Apress, Berkeley, CA, 2017).
- [3] LeCun, Y., Bottou, L., Orr, G. B. & Müller, K. R. Efficient BackProp. In Orr, G. B. & Müller, K.-R. (eds.) *Neural Networks: Tricks of the Trade*, Lecture Notes in Computer Science, 9–50 (Springer Berlin Heidelberg, Berlin, Heidelberg, 1998).
- [4] Tan, T. G., Teo, J. & Anthony, P. A comparative investigation of non-linear activation functions in neural controllers for search-based game AI engineering. *Artificial Intelligence Review* **41**, 1–25 (2014).
- [5] Han, J. & Moraga, C. The influence of the sigmoid function parameters on the speed of backpropagation learning. In Mira, J. & Sandoval, F. (eds.) *From Natural to Artificial Neural Computation*, Lecture Notes in Computer Science, 195–201 (Springer, Berlin, Heidelberg, 1995).
- [6] Werbos, P. Backpropagation through time: What it does and how to do it. *Proceedings of the IEEE* **78**, 1550–1560 (1990).
- [7] Chibole, J. P. Performance Analysis of the Sigmoid and Fibonacci Activation Functions in NGA Architecture for a Generalized Independent Component Analysis (2017).
- [8] Omidvar, O. & Elliott, D. L. *Neural Systems for Control* (Academic Press, 1997), 1st edn.
- [9] Mostafa, M., Teich, W. G. & Lindner, J. Approximation of activation functions for vector equalization based on recurrent neural networks. In *2014 8th International Symposium on Turbo Codes and Iterative Information Processing (ISTC)*, 52–56 (2014).
- [10] Lipovetsky, S. Double logistic curve in regression modeling. *Journal of Applied Statistics* **37**, 1785–1793 (2010).
- [11] McDowall, L. M. & Dampney, R. A. L. Calculation of threshold and saturation points of sigmoidal baroreflex function curves. *American Journal of Physiology-Heart and Circulatory Physiology* **291**, H2003–H2007 (2006).
- [12] Perna, A. *et al.* Individual Rules for Trail Pattern Formation in Argentine Ants (*Linepithema humile*). *PLOS Computational Biology* **8**, e1002592 (2012).
- [13] Chen, W. *Feedback, Nonlinear, and Distributed Circuits* (CRC Press, 2018).
- [14] Vas, P. *Artificial-Intelligence-Based Electrical Machines and Drives: Application of Fuzzy, Neural, Fuzzy-Neural, and Genetic-Algorithm-Based Techniques*. Monographs in Electrical and Electronic Engineering (Oxford University Press, Oxford, New York, 1999).
- [15] Rairan, J. D. Robot Path Optimization Based on a Reference Model and Sigmoid Functions. *International Journal of Advanced Robotic Systems* **12**, 19 (2015).
- [16] Shao, X. & Wang, H. Nonlinear tracking differentiator based on improved sigmoid function. *Control Theory and Application* **31**, 1116–1122 (20140901).
- [17] Mansor, M. A. & Sathasivam, S. Performance analysis of activation function in higher order logic programming. *AIP Conference Proceedings* **1750**, 030007 (2016).
- [18] Mohammad, D., Elshafie, A. H., Othman, J., Karim, O. A. & Sharifah, M. Comparison of artificial neural network transfer functions abilities to simulate extreme runoff data. *International Proceedings of Chemical, Biological and Environmental Engineering (IPCBBE)* **33**, 39–44 (2012).
- [19] Klimek, M. D. & Perelstein, M. Neural Network-Based Approach to Phase Space Integration. *arXiv:1810.11509 [hep-ex, physics:hep-ph, physics:physics, stat]* (2018). URL <http://arxiv.org/abs/1810.11509>.
- [20] Sartin, M. A. & da Silva, A. C. R. Approximation of hyperbolic tangent activation function using hybrid methods. In *2013 8th International Workshop on Reconfigurable and Communication-Centric Systems-on-Chip (ReCoSoC)*, 1–6 (2013).
- [21] Che-Wei Lin & Jeen-Shing Wang. A digital circuit design of hyperbolic tangent sigmoid function for neural networks. In *2008 IEEE International Symposium on Circuits and Systems*, 856–859 (2008).
- [22] Paralı, L., Sari, A., Kılıç, U., Şahin, Ö. & Pěchoušek, J. The artificial neural network modelling of the piezoelectric actuator vibrations using laser displacement sensor. *Journal of Electrical Engineering* **68**, 371–377 (2017).

- [23] Zamanlooy, B. & Mirhassani, M. Efficient VLSI Implementation of Neural Networks With Hyperbolic Tangent Activation Function. *IEEE Transactions on Very Large Scale Integration (VLSI) Systems* **22**, 39–48 (2014).
- [24] Ohn, I. & Kim, Y. Smooth Function Approximation by Deep Neural Networks with General Activation Functions. *Entropy* **21**, 627 (2019).
- [25] Hochreiter, S. & Schmidhuber, J. Long Short-Term Memory. *Neural Computation* **9**, 1735–1780 (1997).
- [26] Kong, S. & Takatsuka, M. Hexpo: A vanishing-proof activation function. In *2017 International Joint Conference on Neural Networks (IJCNN)*, 2562–2567 (IEEE, Anchorage, AK, USA, 2017).
- [27] Schmidhuber, J. Deep learning in neural networks: An overview. *Neural Networks* **61**, 85–117 (2015).
- [28] Carlile, B., Delamarter, G., Kinney, P., Marti, A. & Whitney, B. Improving Deep Learning by Inverse Square Root Linear Units (ISRLUs). *arXiv:1710.09967 [cs]* (2017). URL <http://arxiv.org/abs/1710.09967>.
- [29] Elliott, D. L. & Elliott, D. L. *A Better Activation Function for Artificial Neural Networks* (1993).
- [30] Jin, X. *et al.* Deep learning with S-shaped rectified linear activation units. In *Proceedings of the Thirtieth AAAI Conference on Artificial Intelligence*, 1737–1743 (2016).
- [31] Goodfellow, I., Warde-Farley, D., Mirza, M., Courville, A. & Bengio, Y. Maxout networks. In *International Conference on Machine Learning*, 1319–1327 (PMLR, 2013).
- [32] Gashler, M. S. & Ashmore, S. C. Training deep fourier neural networks to fit time-series data. *Intelligent Computing in Bioinformatics* **48** (2014).
- [33] Nwankpa, C., Ijomah, W., Gachagan, A. & Marshall, S. Activation Functions: Comparison of trends in Practice and Research for Deep Learning. *arXiv:1811.03378 [cs]* (2018). URL <http://arxiv.org/abs/1811.03378>.
- [34] Bekas, K., Curioni, A., Ineichen, Y. & Malossi, A. C. I. Fast, energy-efficient exponential computations in simd architectures (2016). URL <https://patents.google.com/patent/US20160124713A1/en>.
- [35] Timmons, N. G. & Rice, A. Approximating Activation Functions. *arXiv:2001.06370 [cs, stat]* (2020). URL <http://arxiv.org/abs/2001.06370>.
- [36] Greff, K., Srivastava, R. K., Koutník, J., Steunebrink, B. R. & Schmidhuber, J. LSTM: A Search Space Odyssey. *IEEE Transactions on Neural Networks and Learning Systems* **28**, 2222–2232 (2017).
- [37] Muller, J.-M. Elementary Functions and Approximate Computing. *Proceedings of the IEEE* **1–14** (2020).
- [38] Somefun, O. <https://github.com/somefunAgba/nlogisticsigmoid> (2020). URL <https://github.com/somefunAgba/nlogisticsigmoid>.
- [39] He, K., Zhang, X., Ren, S. & Sun, J. Delving Deep into Rectifiers: Surpassing Human-Level Performance on ImageNet Classification. In *2015 IEEE International Conference on Computer Vision (ICCV)*, 1026–1034 (2015).